HHS Public Access

Author manuscript

Talanta Open. Author manuscript; available in PMC 2024 January 05.

Published in final edited form as:

Talanta Open. 2023 December ; 8: . doi:10.1016/j.talo.2023.100241.

Deconvolution of multichannel LC-MS/MS chromatograms of glucosamine-phosphates: Evidence of a GlmS regulatory difference between *Staphylococcus aureus* and *Enterococcus faecium*

Nitish R. Mishra[1],

Amar Deep Sharma[1],

Shivani Gargvanshi,

William G. Gutheil[*]

Division of Pharmacology and Pharmaceutical Sciences, School of Pharmacy, University of Missouri-Kansas City, Kansas City, MO, 64108, USA

Abstract

Resolving isomeric analytes is challenging given their physical similarity – making chromatographic resolution difficult, and their identical masses – making simple mass resolution impossible. MS/MS data provides a means to resolve isomeric analytes if their MS/MS intensity profiles are sufficiently different. Glucosamine-6-phosphate (GlcN-6P) and glucosamine-1-phosphate (GlcN-1P) are early bacterial cell wall intermediates. These and other isomeric hexosamine-phosphates are highly polar and unretained on reverse-phase chromatography media. Three commercially available hexosamine-phosphate standards (GlcN-6P, GlcN-1P, and GalN-1P) were derivatized with octanoic anhydride, and chromatographic conditions were established to resolve these analytes on C18 columns. GlcN-1P and GalN-1P overlapped chromatographically under all tested chromatography conditions. Three MS/MS fragments (79, 97, and 199 *m/z*) were common to all three commercially available hexosamine-phosphates. Intensity ratios of the three MS/MS fragments from these three hexosamine-phosphate standards were used to deconvolute mixture chromatograms of these standards by non-negative linear regression. This approach allowed the complete resolution of these analytes. The chromatographically overlapping GlcN-1P and GalN-1P, which shared similar but modestly different MS/MS intensity profiles, were fully resolved with this non-negative deconvolution approach. This approach was then applied to MRSA, VSE, and VRE bacterial extracts before and after exposure to vancomycin. This demonstrated a substantial (3-fold) increase in GlcN-6P in vancomycin-treated MRSA samples but not in vancomycin-treated VSE or VRE samples. These observations appear to localize previously

[*]Corresponding author. gutheilw@umkc.edu (W.G. Gutheil).

[1]These authors contributed equally to this work.

Declaration of Competing Interest

The authors declare that they have no known competing financial interests or personal relationships that could have appeared to influence the work reported in this paper.

Supplementary materials

Supplementary material associated with this article can be found, in the online version, at doi:10.1016/j.talo.2023.100241.

observed differences between MRSA and VRE/VSE peptidoglycan biosynthesis regulation to GlmS, which synthesizes GlcN-6P and is the product of a regulatory ribozyme sensitive to the levels of GlcN-6P

Keywords

Glucosamine-6-phosphate; Glucosamine-1-phosphate; Galactosamine-1-phosphate; LC-MS/MS; Peptidoglycan; GlmS; Non-negative deconvolution

1. Introduction

Glucosamine-6-phosphate (GlcN-6P) and glucosamine-1-phosphate (GlcN-1P) are early intermediates in amino sugar biosynthesis and are the immediate precursors to uridine diphosphate N-acetylglucosamine (UDP-NAG) in the bacterial cell wall peptidoglycan biosynthesis pathway (Fig. 1) [1–5].

Bacterial cell wall biosynthesis is the target of many of our most effective antibiotics, and these early steps may be good targets for new antibacterial agent development efforts [6–9]. The ability to detect and quantify these intermediates in biological samples is necessary for assessing the regulation of the peptidoglycan biosynthesis pathway in bacteria and the effect of peptidoglycan biosynthesis inhibitors on their levels. A variety of methods for detecting and quantifying glucosamine and galactosamine have been described. These include the classical colorimetric Elson and Morgan method based on the reaction of glucosamine and galactosamine with acetylacetone and *p*-dimethylaminobenzaldehyde (Ehrlich's reagent) [10] and variations on this method [11]. More recently, LC-MS/MS methods with and without chemical derivatization have been developed for glucosamine and galactosamine [12,13]. Quantifying these glucosamine phosphates and related hexosamine phosphates in biological samples has proven substantially more challenging. Classic studies used ion exchange separations, followed by hydrolysis and Elson-Morgan derivatization, to identify glucosamine phosphates [14]. A more recent study used the GlmS ribozyme's sensitivity to GlcN-6P as the basis for a fluorescence resonance energy transfer-based assay for GlcN-6P [15]. An LC-MS/MS approach to hexosamine phosphates would seem ideal but is complicated by their high polarity and correspondingly poor retention on reverse-phase HPLC columns commonly used in LC-MS analytical analyses. There are also several highly similar hexosamine phosphate isomers, such as GlcN-1P, GlcN-6P, galactosamine-1P (GalN-1P), galactosamine-6P (GalN-6P), as well as potential α- and β-anomers of the hexosamine-6-phosphates. These features complicate the resolution and individual quantification of these key analytes in complex mixtures.

In this study, we develop an LC-MS/MS assay for hexosamine phosphates using an alkanoic anhydride precolumn derivatization strategy. Three amine derivatization strategies were tested: hexanoic anhydride, octanoic anhydride, and decanoic anhydride. All three gave nearly identical results, and this report focuses on the representative octanoic anhydride derivatization strategy. The resulting amine octanoate derivatives were well retained on reverse-phase HPLC media, and each of the three commercially available standards (GlcN-6P, GlcN-1P, and GalN-1P) gave the same three MS/MS fragments (79, 97, and

199 *m/z*) in differing ratios. The ratio differences between these three analytes allowed for their linear deconvolution to resolve overlapping chromatographic peaks. This approach was then demonstrated for determining the levels of these intermediates in methicillin-resistant *Staphylococcus aureus* (MRSA), vancomycin-resistant *Enterococcus faecium* (VRE), and vancomycin-sensitive *Enterococcus faecium* (VSE) before and after vancomycin treatment. This revealed a sharp increase in GlcN-6P levels in MRSA upon vancomycin exposure but not in VRE or VSE. This parallels the observed accumulation of UDP-linked peptidoglycan intermediates in MRSA upon exposure to vancomycin [16] and the lack of UDP-linked accumulation in VRE and VSE upon vancomycin exposure [17]. These observations suggest a difference between MRSA and VRE/VSE in GlmS, which regulates entry into the bacterial peptidoglycan biosynthesis pathway in the form of an mRNA ribozyme riboswitch which self-inactivates in the presence of GlcN-6P – its immediate product [5,8,9,18].

2. Materials and methods

2.1. General materials and reagents

GlcN-1P, GlcN-6P, GalN-1P, octanoic anhydride, and triethylamine were purchased from Millipore-Sigma. LC-MS grade water with 0.1% formic acid was from Fisher Scientific. LC-MS grade acetonitrile (ACN) with 0.1% formic acid was from Honeywell, Riedel-de. LC-MS grade isopropyl alcohol, water, and acetonitrile were from Honeywell, Burdick & Jackson™ (Muskegon, MI). LC-MS grade formic acid (FA) and Mueller Hilton Broth 2 (cation adjusted) were from Millipore Sigma (Darmstadt, Germany). LC-MS-grade methanol was from Alfa Aesar (Ward Hill, MA). Roc C18 HPLC column, 5 μm, 150 × 3.0 mm, was from Restek. Centrifuge operations were performed in an Eppendorf 5424 centrifuge. LC-MS analyses were performed on an AB Sciex 3200 QTrap mass spectrometer (Foster City, CA) coupled to a Shimadzu UFLC system (Columbia, MD) using electrospray ionization (ESI) and run with Analyst v.1.4.2 software.

2.2. Derivatization of GlcN-1P, GlcN-6P, and GlcN-1P standards

Hexosamine-phosphates are highly polar and poorly retained on reverse-phase chromatography media. To overcome this problem, commercially available hexosamine-phosphates (GlcN-6P, GlcN-1P, and GalN-1P) were amine derivatized using octanoic anhydride. Reactions were conducted by mixing a 20 μL aliquot of each hexosamine-phosphate standard at 250 μM with 40 μL of 20 mM of octanoic anhydride in acetone, followed by the addition of 10 μL of 0.5 M triethylamine (TEA) in water to initiate the reaction. The reaction mixtures were incubated at 35 °C for 2 hrs. The derivatization reactions were quenched by adding 10 μL of 0.5 M HCl in water. The samples were diluted to 200 μL with 10% acetonitrile/0.1% formic acid to make a nominal concentration of each standard at 25 μM.

2.3. LC-MS/MS method development

Pure standard samples derivatized with octanoic anhydride were tuned for MS/MS detection and quantification by infusion using the Analyst software Quantitative Optimization Wizard. There were three commercially available analytes for this effort (GlcN-1P, GlcN-6P, and GalN-1P), each with the same three major fragments (79, 97, 199). For each derivative,

a consensus set of MS/MS detection parameters was selected for each common fragment (octanoate derivative parameters given in Table 1). Liquid chromatographic (LC) separations were performed on a Restek Roc C18 150 × 3.0 mm, 5 μm column. LC solvents were 0.1% formic acid in water (solvent A) and 0.1% formic acid acetonitrile (solvent B). The LC gradient was 5% B (0–1 min), 5–50% B (1–21 min), 50–95% B (21–22 min), 95% B (22–23 min), 95–5% B (23–24 min), and 5% B (24–30 min). The three derivatization approaches (hexanoate, octanoate, and decanoate) gave similar results. This report is therefore focused on the octanoate derivatives.

2.4. Data import

Data files were converted from the Analyst WIFF data format to the NetCDF format using the Analyst Translat.exe utility. Data in the NetCDF files were imported into a MATLAB data structure using MATLAB's NetCDF file functions. Each of the three MS/MS fragment channel data was collected discretely for 200 msec, and the second and third MS/MS data channels are therefore offset by 200 and 400 msec from the time value. The MATLAB cubic spline function (spline) was used to realign the data from each MS channel to the same time vector. This has a modest but detectable effect on data deconvolution. Raw data for the three standards is shown in Fig. 2, left panels.

2.5. Data reweighting

This analysis depends on the difference between the analyte MS/MS fragment intensities of different analytes. A characteristic of MS/MS signals is that they have the same relative error over a wide range of signal intensities. In the least squares analyses, it is common to reweight the data so that different data points have weights proportional to their relative errors rather than simply to their magnitudes. This study's three-channel MS/MS data (79, 97, 199 *m/z*) was reweighted by calculating a reweighting factor to equal the sum of the channel's intensities across all three standards. Reweighted raw data for these standards is shown in the central column of Fig. 2. Intensity changes and values for reweighting the three standards are shown in Fig. 3. Note that this dramatically enhances the differences in MS/MS signal intensities, particularly between GlcN-1P and GalN-1P (Fig. 3).

2.6. Non-negative linear deconvolution

Our approach to non-negative linear deconvolution of multichannel MRM data has been described previously [19]. The 3 MS fragments (channels) used in this study demonstrated different intensity ratios for the hexosamine-phosphate isomers. This allows the deconvolution of overlapping peaks into their components using a linear least squares approach. The expected multichannel chromatogram can be predicted given A – an n x m matrix with m columns for each pure standard, n rows for each MS/MS fragment channel, and x – an m x t matrix of the concentrations of each component as a function of time. The predicted n x t multichannel MS chromatogram b is then given by:

$$Ax = b \tag{1}$$

Since the intensity profile of the pure components (A) can be determined directly from LC-MS/MS chromatograms of the pure (well-resolved) components. The observed multichannel chromatogram (b) of an overlapping mixture can be linearly deconvoluted in the least squares sense to give the component concentrations (x) vs. t profiles using the MATLAB backslash operator-based formula:

$$x = A\backslash b \tag{2}$$

However, a problem with direct linear deconvolution is that negative component concentrations may be predicted, which are physically meaningless. The need for non-negative solutions in multivariate analyses is a common problem, and general approaches to non-negative least squares (NNLS) – where solutions to x in Eq. 4 are constrained to have values ≥ 0, are implemented in several analysis packages, including MATLAB. As implemented in a prior study [19], the MATLAB implementation of NNLS is for problems where both x and b are vectors, whereas the present case required a solution where x and b are both matrices. To address the need of the present analysis, the MATLAB lsqnonneg function was used with iteration over the time dimension in the data matrix (b) to provide the deconvoluted (x) matrix:

$$\begin{array}{l} for\, i = 1 : size(b, 2) \\ x(:, i) = lsqnonneg\ (A, b(:, i)) \\ \text{end} \end{array} \tag{Eq. 3}$$

where A is again the intensity vs. species matrix (Eqs. 3 & 4) determined from LC-MS/MS chromatograms of pure (well-resolved) standards. Application of this approach to the reweighted GlcN-1P, GlcN-6P, and GalN-1P standards data gives the well-resolved deconvoluted standards chromatograms (Fig. 2, left column).

2.7. Bacterial cell extract and matrix preparation

To test the potential of this approach to measuring these analytes in biological samples, and given our interest in inhibitors of bacterial cell wall biosynthesis, we applied this approach to assess the effect of vancomycin exposure on early intermediates in bacteria upon exposure to vancomycin [16,17]. MRSA growth, vancomycin treatment, and metabolite extraction were performed as described in detail previously [16]. VRE and VSE growth, vancomycin treatment, and metabolite extraction were also performed as described previously [17]. Briefly, fresh log phase cultures were grown to 0.4 OD_{600} and divided into two sets of four samples of 15 mL in 50 mL falcon tubes. One set of four was left untreated, and to the other set of four was added 4xMIC of vancomycin. After 15 mins, the control and antibiotic treatment groups were quenched in an ice-cold slush bath for 10 min. The samples were centrifugated at 3300 rpm, and the supernatants were discarded. Bacterial cells were resuspended using 1 mL of ice-cold water and were transferred to 50 mL centrifuge tubes containing 5.5 mL of ice-cold methanol/water/formic acid (80:19.9:0.1). Samples were kept on ice for 5 min with regular vortexing and then centrifuged at 3300 rpm, and the supernatant was collected (first extract) in fresh 50 mL falcon tubes. The pellet was reconstituted with 2 mL of ice-cold methanol/water/formic acid (67:32.9:0.1) and then centrifuged at 3300 rpm, and the supernatant was collected (second extract). The first and

second extracts were combined, 5 mL of LC-MS grade water was added, and the samples were frozen at −80 °C. Samples were lyophilized and then dissolved in 200 μL of 10% acetonitrile/water/0.1% formic acid.

2.8. Derivatization of bacterial extracts and LC-MS/MS analysis

A 10 μL aliquot of each sample was diluted 16 times by adding 150 μL of 5% acetonitrile/water/0.1% formic acid. A 20 μL aliquot of this diluted sample was mixed with 40 μL of 20 mM octanoic anhydride prepared in acetone, followed by 5 μL of 0.5 M triethylamine (TEA) to initiate the reaction. The contents were mixed and kept in the dark at 35 °C for 2 hr. Finally, the reaction mixture was quenched by adding 5 μL of 0.5 M HCl, and the sample was diluted to 200 μL with 10% acetonitrile/0.1% formic acid. Aliquotes of 5 μL of these samples were injected for LC-MS/MS analysis. Data we exported to MATLAB as described above, normalized, and deconvoluted as described above. The results are shown in Fig. 4.

2.9. Linearity and matrix analysis

GlcN-1P, GlcN-6P, and GalN-1P standards were derivatized using octanoic anhydride. These samples were serially diluted in steps of 2 from 1000 pmol to 0.001 pmol, either in 10% acetonitrile, 90% water, 0.1% formic acid (water), or MRSA extract prepared as described above (matrix). The results are shown in Fig. S2 and demonstrate excellent linearity and lack of matrix effect for these analytes.

2.10. Analysis of deconvolution accuracy

GlcN-1P, GlcN-6P, and GalN-1P standards were derivatized using octanoic anhydride as described above. These samples were diluted to achieve a 2.5 μM concentration for each standard and subsequently prepared in a 1:1:1 mix at 2.5 μM for each analyte. The resulting derivatized analytes were then analyzed by LC-MS and then deconvoluted to assess the reproducibility and accuracy of deconvolution (Table 2). The analysis used a 10% acetonitrile and 90% water solution containing 0.1% formic acid.

2.11. Analysis of extraction recovery

Bacteria were grown and extracted with methanol as described above, except that extraction was performed three times, and each extract was kept and analyzed separately. A first:second:third extract ratio of 98.5:1.4:0.05 was observed for all three metabolites (GlcN-1P, GlcN-6P, and GalN-1P). Therefore, the combined two extract procedure used in this study provides a 99.9% analyte recovery.

3. Results and discussion

Bacterial cell wall biosynthesis involves a series of steps, first in the cytoplasm [6] and then within the bacterial cell membrane [20]. In previous studies, we have developed LC-MS/MS assays for all of the UDP-linked intermediates in this pathway [21] and applied them to investigate the effects of antibiotics on the cytoplasmic intermediates in MRSA [22] and vancomycin-resistant and sensitive *Enterococcus faecium* (VRE and VSE) [17]. An interesting observation made in these studies was that blocking the later steps of peptidoglycan biosynthesis in MRSA resulted in a massive accumulation of UDP-linked

cytoplasmic intermediates [16] but not in VRE or VSE [17]. These observations clearly indicate a major difference in how peptidoglycan biosynthesis is regulated between *S. aureus* and *E. faecium*. However, in these studies, we were unable to quantify the levels of GlcN-6P and GlcN-1P, the first intermediates in this pathway (Fig. 1), due to a lack of appropriate analytical methods.

GlcN-6P and related sugar amine phosphates are highly polar and, therefore, unretained on reverse-phase media. This group of agents also have identical masses and similar structures, complicating their separation, detection, and discrimination by LC-MS/MS or other detection methods. The goal of this study was to test and demonstrate an octanoic anhydride amine derivatization-based LC-MS/MS analytical method for resolving these analytes, particularly GlcN-6P and GlcN-1P Three hexosamine phosphates are commercially available – GlcN-1P, GlcN-6P, and GalN-1P – and these were derivatized with octanoic anhydride to provide their corresponding amine octanoate derivatives. These derivatized standards were then used to develop the negative mode MS/MS-based detection and quantification part of this method. All three analytes provided the same three predominant MS/MS fragments (79, 97, and 199 *m/z*). The 79 *m/z* fragment is ascribed to PO_3^- (HRMS gives 78.9582 *m/z*), the 97 *m/z* fragment to $H_2PO_4^-$ (HRMS gives 96.9688 *m/z*), and the 199 *m/z* fragment to $C_4H_8O_7P^-$ (HRMS gives 199.0002 *m/z*). Consensus MS/MS parameters from these three analytes for these three MS/MS fragments were selected for this effort (Table 1).

HPLC separation conditions were then optimized for these three analytes (Fig. 2). Octanoate-derivatized GlcN-1P and GalN-1P always overlapped chromatographically (as did hexanoate and decanoate derivatives). Since GlcN-1P and GalN-1P have only an α isomer, they also showed only a single chromatographic peak (Fig. 2). However, GlcN-6P has both α- and β-anomers (Fig. 1) and showed two chromatographic peaks (Fig. 2). The fragmentation patterns of the two anomer peaks for GlcN-6P were indistinguishable. The larger 13.5 min peak is tentatively identified as the β-anomer, and the earlier smaller 13.0 min peak is tentatively identified as the α-anomer based on a recent NMR study [23].

The linear deconvolution approach requires differences in the MS/MS fragmentation intensities between species for deconvolution to work. While such a difference is apparent in the raw data (Fig. 2 left column and Fig. 3A), some MS/MS signals were of low intensity. A characteristic of MS/MS data is that large signals and small signals tend to have the same relative errors and, therefore, much different absolute errors. It is common in least squares analysis to reweight the data to normalize to the relative data errors, which was done for this study as illustrated in Fig. 2 center column and Fig. 3B. *This key step substantially improved the final deconvolution* (Fig. 2, right column). (Note that the selection of collision energy is also important in providing suitable MS/MS signal intensity differences necessary for successful signal deconvolution (Fig. S1).) Non-negative linear deconvolution can then be used to extract individual component chromatograms (Fig. 2 right column). As illustrated in the lower right panel of Fig. 2, this approach resolves the chromatographically overlapping MS/MS patterns of GlcN-1P and GalN-1P

To assess the inherent error associated with deconvolution. Three pure individual analytes (GlcN-1P, GlcN-6P, and GalN-1P) and a mixture chromatogram were collected in quadruplicate. The deconvolution of these replicates allowed the reproducibility of the deconvolution process to be assessed (Table 2). The deconvolution of pure standards gave relative errors in the 2–3% range, consistent with the injection reproducibility of this LC-MS instrument. In the mixture sample, the well-resolved GlcN-6P peak also gave a low relative error of ~1%. Deconvolution of the overlapping GlcN-1P and GalN-1P peaks gave higher relative errors of 5–8%, which are still acceptable for bioanalytical studies.

The optimized LC-MS/MS method was tested for linearity and lack of matrix effects, which were both excellent (Fig. S2). This method was then applied to biological samples. MRSA, VRE, and VSE without and with vancomycin treatment were prepared and analyzed (Fig. 4).

Relatively weak but detectable signals were observed for GlcN-1P (red peak at 11.2 min), which is not unexpected since it is a high-energy intermediate. GalN-1P was absent from these samples. In MRSA samples, the deconvoluted chromatograms show the expected GlcN-6P anomer peaks at 13 and 13.5 min, but also a new set of earlier eluting anomer peaks in the “GlcN-6P channel” at 11.5 to 12.0 min. Only three hexosamine sugars are commonly observed in nature, GlcN, GalN, and mannosamine (ManN). The unknown peaks seem unlikely to be from GalN-6P since we do not observe any corresponding GalN-1P peak (unfortunately, while we have a commercial standard for GalN-1P, we were unable to find a standard for GalN-6P). MRSA is known to use *N*-acetyl-mannosamine for teichoic acid biosynthesis [24]. However, the UDP-ManNAc used for teichoic acid biosynthesis is derived directly from UDP-NAG [1], not ManN-6P The unidentified “GlcN-6P channel” peaks at 11.5 and 12.0 min may be ManA-6P from a mannosamine salvage pathway. VSE and VRE also show an unknown peak in the GlcN-1P channel at 13.3 min and two closely spaced unknown peaks in the GalN-1P channel at 13.5 and 13.6 min.

MRSA samples demonstrated a nearly 3-fold increase in the GlcN-6P anomer peaks eluting at 13 and 13.5 min, whereas VRE and VSE demonstrated a no or very small increase (Fig. 4). In MRSA, this is accompanied by no change or a small decrease in the mystery “GlcN-6P channel” (possibly ManA-6P) anomer peaks (11.5 and 12.0 min). This observation of a substantial increase in the GlcN-6P levels in MRSA but not in VRE or VSE upon vancomycin exposure parallels the observation of large UDP-linked intermediate accumulation in MRSA upon vancomycin exposure [16] and the lack of UDP-linked intermediate accumulation in VRE or VSE upon vancomycin treatment [17]. The results of this method development and demonstration study suggest that the difference between MRSA and *Enterococcus faecium* may be in the first enzyme in the peptidoglycan biosynthesis pathway, GlmS. GlmS is a known regulatory point for peptidoglycan synthesis in Gram-positive bacteria in the form of an mRNA ribozyme that self-inactivates in the presence of its catalytic product, GlcN-6P [5,18,25]. Using a deconvoluted standard mix as a reference and the optical density-cell mass-cell volume relationships in MRSA as described previously [16], the concentrations of these intermediates in MRSA and VRE were calculated (Table 3).

Supplementary Material

Refer to Web version on PubMed Central for supplementary material.

Funding

This work was supported by National Institutes of Health Grant R15 GM126502 (to W.G.).

Data availability

Data will be made available on request.

References

[1]. Kawamura T, Kimura M, Yamamori S, Ito E, Enzymatic formation of uridine diphosphate N-acetyl-D-mannosamine, J. Biol. Chem. 253 (10) (1978) 3595–3601. [PubMed: 418068]

[2]. Milewski S, Glucosamine-6-phosphate synthase–the multi-facets enzyme, Biochim. Biophys. Acta 1597 (2) (2002) 173–192. [PubMed: 12044898]

[3]. Teplyakov A, Leriche C, Obmolova G, Badet B, Badet-Denisot MA, From Lobry de Bruyn to enzyme-catalyzed ammonia channelling: molecular studies of D-glucosamine-6P synthase, Nat. Prod. Rep. 19 (1) (2002) 60–69. [PubMed: 11902440]

[4]. Komatsuzawa H, Fujiwara T, Nishi H, Yamada S, Ohara M, McCallum N, Berger-Bachi B, Sugai M, The gate controlling cell wall synthesis in Staphylococcus aureus, Mol. Microbiol. 53 (4) (2004) 1221–1231. [PubMed: 15306023]

[5]. Winkler WC, Nahvi A, Roth A, Collins JA, Breaker RR, Control of gene expression by a natural metabolite-responsive ribozyme, Nature 428 (6980) (2004) 281–286. [PubMed: 15029187]

[6]. Barreteau H, Kovac A, Boniface A, Sova M, Gobec S, Blanot D, Cytoplasmic steps of peptidoglycan biosynthesis, FEMS Microbiol. Rev. 32 (2) (2008) 168–207. [PubMed: 18266853]

[7]. Rani C, Khan IA, UDP-GlcNAc pathway: potential target for inhibitor discovery against M. tuberculosis, Eur. J. Pharm. Sci. 83 (2016) 62–70. [PubMed: 26690048]

[8]. Sachla AJ, Helmann JD, Resource sharing between central metabolism and cell envelope synthesis, Curr. Opin. Microbiol. 60 (2021) 34–43. [PubMed: 33581378]

[9]. Wyllie JA, McKay MV, Barrow AS, Soares da Costa TP, Biosynthesis of uridine diphosphate N-Acetylglucosamine: an underexploited pathway in the search for novel antibiotics? IUBMB Life 74 (12) (2022) 1232–1252. [PubMed: 35880704]

[10]. Blix G, The determination of hexosamines according to Elson and Morgan, Acta Chem. Scand. 2 (1948) 467–473.

[11]. Roseman S, Daffner I, Colorimetric method for determination of glucosamine and galactosamine, Anal. Chem. 28 (11) (1956) 1743–1746.

[12]. Song M, Hang TJ, Wang C, Yang L, Wen AD, Precolumn derivatization LC-MS/MS method for the determination and pharmacokinetic study of glucosamine in human plasma and urine, J. Pharm. Anal. 2 (1) (2012) 19–28. [PubMed: 29403716]

[13]. Olofsson MA, Bylund D, Liquid chromatography with electrospray ionization and tandem mass spectrometry applied in the quantitative analysis of chitin-derived glucosamine for a rapid estimation of fungal biomass in soil, Int. J. Anal. Chem. 2016 (2016), 9269357. [PubMed: 26977151]

[14]. Pogell BM, Gryder RM, Enzymatic synthesis of glucosamine 6-phosphate in rat liver, J. Biol. Chem. 228 (2) (1957) 701–712. [PubMed: 13475353]

[15]. Furchak JR, Yang P, Jennings C, Walter NG, Kennedy RT, Assay for glucosamine 6-phosphate using a ligand-activated ribozyme with fluorescence resonance energy transfer or CE-laser-induced fluorescence detection, Anal. Chem. 80 (21) (2008) 8195–8201. [PubMed: 18842060]

[16]. Vemula H, Ayon NJ, Burton A, Gutheil WG, Antibiotic effects on methicillin-resistant staphylococcus aureus cytoplasmic peptidoglycan intermediate levels and evidence for potential metabolite level regulatory loops, Antimicrob. Agents Chemother. 61 (6) (2017).

[17]. Gargvanshi S, Vemula H, Gutheil WG, Effect of vancomycin on cytoplasmic peptidoglycan intermediates and van operon mRNA levels in VanA-type vancomycin-resistant enterococcus faecium, J. Bacteriol. 203 (16) (2021), e0023021. [PubMed: 34060906]

[18]. Richards J, Belasco JG, Riboswitch control of bacterial RNA stability, Mol. Microbiol. 116 (2) (2021) 361–365. [PubMed: 33797153]

[19]. Vemula H, Kitase Y, Ayon NJ, Bonewald L, Gutheil WG, Gaussian and linear deconvolution of LC-MS/MS chromatograms of the eight aminobutyric acid isomers, Anal. Biochem. 516 (2017) 75–85. [PubMed: 27771391]

[20]. van Heijenoort J, Lipid intermediates in the biosynthesis of bacterial peptidoglycan, Microbiol. Mol. Biol. Rev. 71 (4) (2007) 620–635. [PubMed: 18063720]

[21]. Vemula H, Bobba S, Putty S, Barbara JE, Gutheil WG, Ion-pairing liquid chromatography-tandem mass spectrometry-based quantification of uridine diphosphate-linked intermediates in the Staphylococcus aureus cell wall biosynthesis pathway, Anal. Biochem. 465 (2014) 12–19. [PubMed: 25086364]

[22]. Vemula H, Ayon NJ, Gutheil WG, Cytoplasmic peptidoglycan intermediate levels in Staphylococcus aureus, Biochimie 121 (2016) 72–78. [PubMed: 26612730]

[23]. Virués C, Hernández J, Higuera-Ciapara I, Martínez-Benavidez E, Olivares-Romero JL, Navarro RE, Inoue M, Formulation of anomerization and protonation in D-glucosamine, based on (1)H NMR, Carbohydr. Res. 490 (2020), 107952. [PubMed: 32114014]

[24]. Brown S, Santa Maria JP Jr., S. Walker, Wall teichoic acids of gram-positive bacteria, Annu. Rev. Microbiol. 67 (2013) 313–336. [PubMed: 24024634]

[25]. Panchal V, Brenk R, Riboswitches as Drug Targets for Antibiotics,, Antibiotics (Basel) 10 (1) (2021).

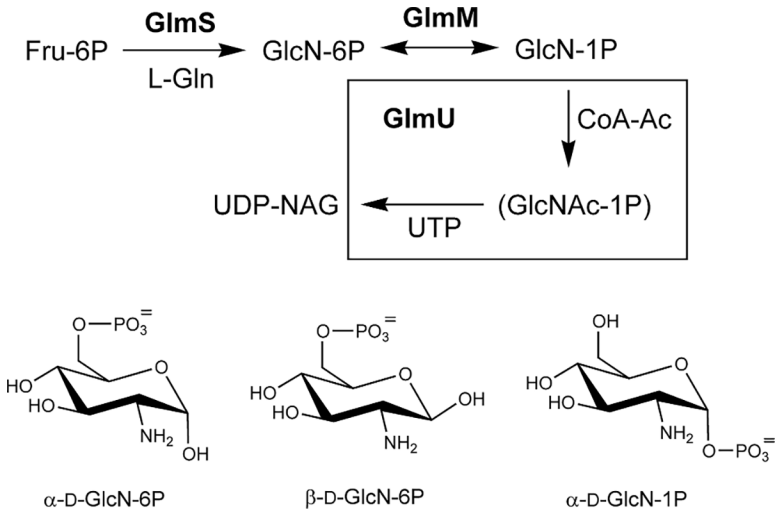

Fig. 1.

Top: Early steps in the bacterial cell wall biosynthesis pathway leading to UDP-NAG. GlmU is a bifunctional enzyme, as indicated with the boxed reactions. Bottom: Pyranose structures of the two anomeric (α and β) D-GlcN-6P isomers and the α-D-GlcN-1P isomer.

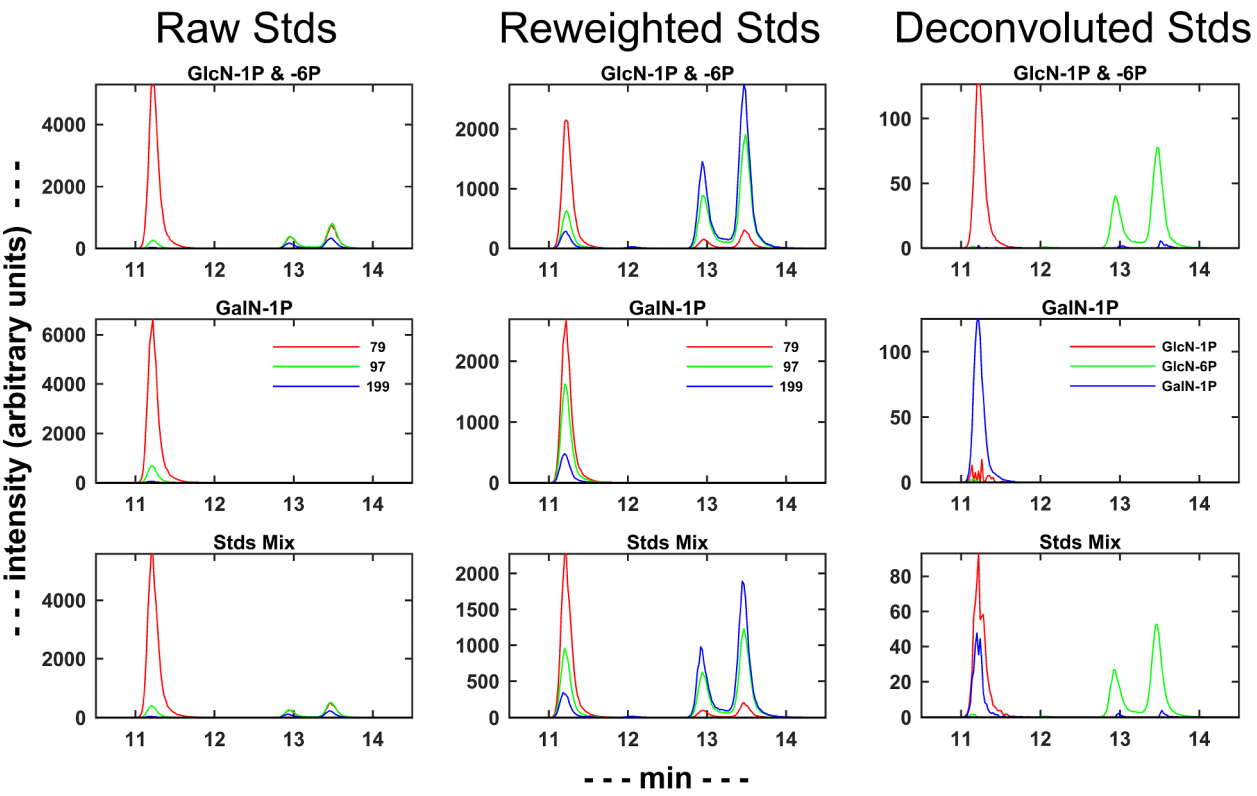

Fig. 2.

Raw and processed standards data. Identifications given in the middle panel insets. From left to right: Left column panels: Raw octanoate derivative MS/MS data, Center column panels: Reweighted MS/MS data; Right column panels: Deconvoluted reweighted MS/MS data into relative species concentrations. From top to bottom: Top row panels: Mixture of GlcN-1P (peak at 11.2 min) and GlcN-6P (two peaks for the α- and β-anomers between 13 and 13.5 min). Middle row panels: GalN-1P (peak also at 11.2 min). Bottom row panels: Mixture of all three analytes – GlcN-1P, GlcN-6P, and GalN-1P Note that in the lower right panel all three of these analytes can be fully resolved using a combination of chromatographic separation and MS/MS signal deconvolution.

A

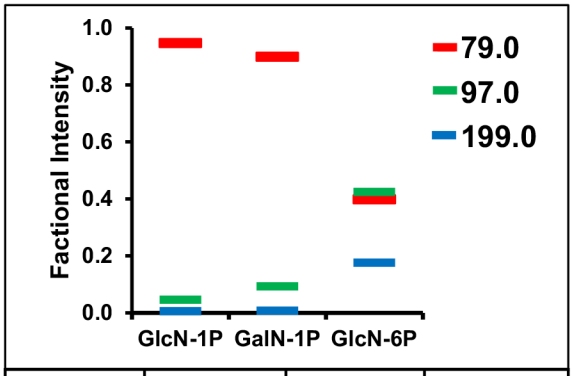

MS/MS (m/z)	GlcN-1P	GalN-1P	GlcN-6P
79.0	0.947	0.899	0.399
97.0	0.047	0.093	0.425
199.0	0.006	0.008	0.177

B

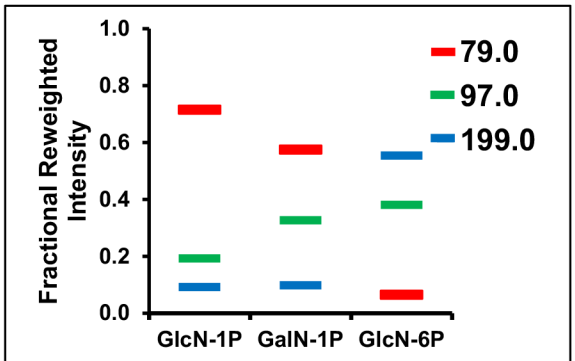

MS/MS (m/z)	GlcN-1P	GalN-1P	GlcN-6P
79.0	0.715	0.575	0.065
97.0	0.193	0.327	0.381
199.0	0.092	0.098	0.554

Fig. 3.

A: Intensity profile for octanoate derivatize analytes as fractions of the total (summed) intensity of the three MS/MS fragment channels. Bars represent fraction of intensity for that analyte (x-axis). B: Reweighted fractional intensity profiles. Reweighting was performed to make the summed *total* signal intensity for each MS/MS fragment channel the same for these three standards. Below each panel are the fractional signal intensities before (A) and after (B) reweighting.

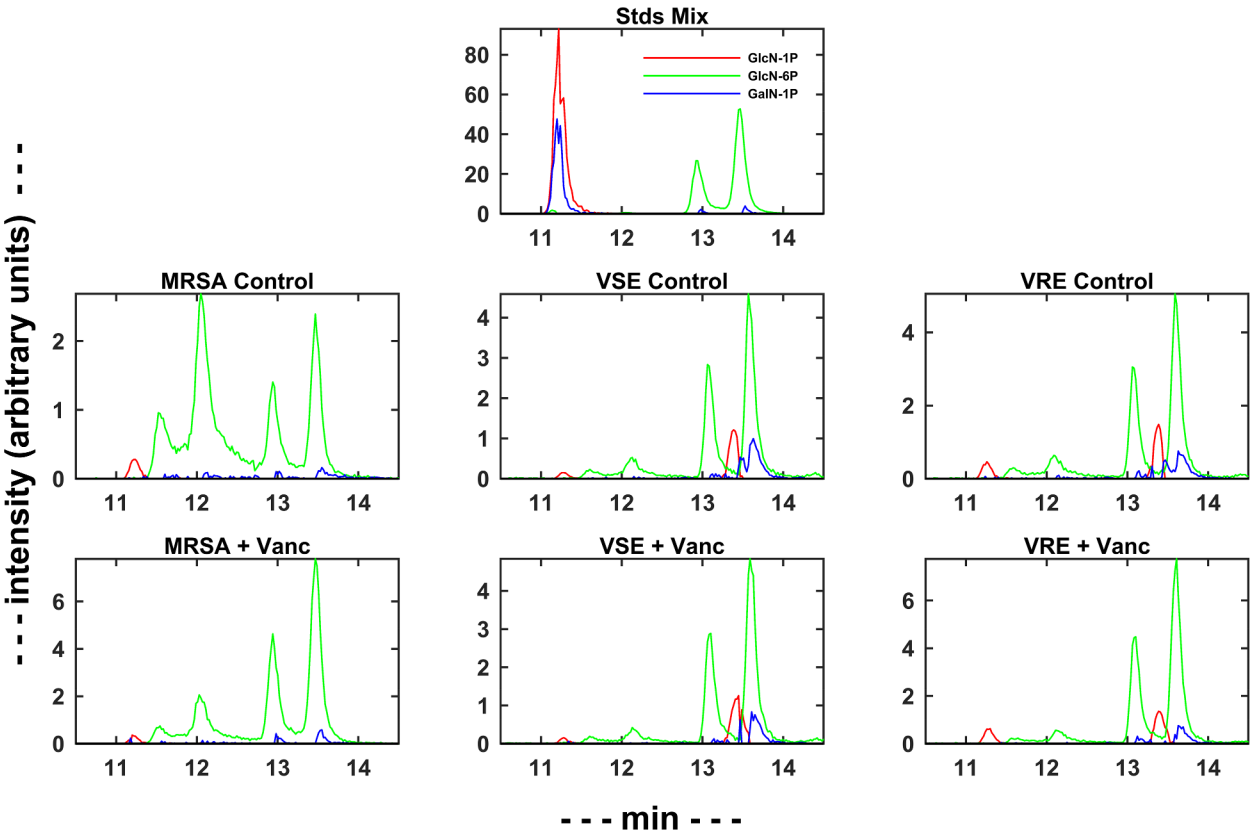

Fig. 4.

Deconvoluted LC-MS/MS chromatograms demonstrating application of the hexosamine phosphate MS/MS deconvolution approach to biological samples. The top panel shows the deconvoluted octanoate derivatized standard mix. Middle row panels show deconvoluted chromatograms from MRSA (left), VSE (middle), and VRE (right). The bottom sets of panels show the effect of added vancomycin. Note that there are some unidentified peaks in the MRSA sample in the GlcN-6P “channel” (leftmost green peaks at 11.5 and 12 min), likely due to mannosamine phosphate in MRSA. There are traces of GlcN-1P, no detectible levels of GalN-1P, and other minor unidentified peaks in these biological samples. The peak for GlcN-6P in MRSA is about 3-fold higher in the vancomycin-treated sample than in the control sample. No similar increase is seen in the vancomycin-treated VSE or VRE samples.

Table 1

LC-MS/MS detection parameters for the most intense MS/MS negative mode transitions of the three commercially available hexosamine phosphates after amine derivatization with octanoic anhydride.

Q1	Q3	DP	EP	CEP	CE
384.1	79.0	− 75	− 9.25	− 16	− 70
	97.0				− 31
	199.0				− 22

Q1, parent ion; Q3, product ion; DP, source declustering potential; EP, source entrance potential; CEP, collision cell entrance potential; CE, collision cell collision energy. Other ion path parameters at instrument defaults. For all ions: collisionally activated dissociation (CAD) gas level, arbitrary units = high; source temperature = 450 °C; curtain gas setting = 20 psi; gas flow 1 setting = 50 psi; gas flow 2 setting = 50 psi.

Table 2

Deconvolution accuracy.

Sample	Deconvoluted Species	Replicate[a] 1	2	3	4	Avg	SD	%RE
GlcN-1P Std	GlcN-1P	0.948	0.965	0.987	1.012	0.978	0.028	2.85
	GlcN-6P	0.001	0.001	0.001	0.001			
	GalN-1P	0.022	0.027	0.030	0.035			
GlcN-6P Std	GlcN-1P	0.000	0.000	0.000	0.000			
	GlcN-6P	1.002	0.971	0.989	1.018	0.995	0.020	2.00
	GalN-1P	0.001	0.001	0.001	0.001			
GalN-1P Std	GlcN-1P	0.068	0.088	0.078	0.085			
	GlcN-6P	0.002	0.002	0.001	0.001			
	GalN-1P	0.917	0.865	0.857	0.884	0.881	0.026	3.00
Std Mix (1:1:1)	GlcN-1P	0.975	0.880	0.916	1.064	0.959	0.080	8.39
	GlcN-6P	1.094	1.119	1.111	1.124	1.112	0.013	1.19
	GalN-1P	1.128	1.176	1.195	1.045	1.136	0.067	5.91

[a]All standard and standard mix solutions were at 2.5 μM for each octanoic anhydride derivatized analyte. LC-MS analysis was performed using 10 μL injections (25 pmol). Deconvoluted signal areas are relative to the average corresponding standard signal intensity given the deconvolution procedure, such that the deconvoluted area for each analyte should be ~1.0 (1.0 area units/25 pmol).

Table 3

Intracellular concentrations of analytes.

	µM in cells GlcN-1P	GlcN-6P	GalN-1P
MRSA Control	110	1800	40
MRSA + Vanc	120	5800	70
VSE Control	60	3100	10
VSE + Vanc	50	3400	20
VRE Control	170	3400	30
VRE + Vanc	250	5200	30